Supporting Information

for

Encapsulating Low-Coordinated Pt Clusters within a Metal-Organic Framework Induces Spatial Charge Separation Boosting Photocatalytic Hydrogen Evolution

Yao-Yao Wang,[a] Zheng Tang,[a] Xue-Yang Ji,[a] Song Wang,*[b] Zi-Shuo Yao*[a] and Jun Tao*[a]

[a] Key Laboratory of Cluster Science of Ministry of Education, School of Chemistry and Chemical Engineering, Liangxiang Campus, Beijing Institute of Technology, Beijing 102488, P. R. China

[b] Hubei Key Laboratory of Low Dimensional Optoelectronic Materials and Devices, Hubei University of Arts and Science, Xiangyang, Hubei 441053, P. R. China

E-mail: taojun@bit.edu.cn; zishuoyao@bit.edu.cn; wangsong1984@126.com.

Table of Contents

Table S1. ICP-MS analysis of catalysts

Sample	Pt wt%	H_2 evolution rate (μmol g^{-1} h^{-1})
U6N	0	1.03
Pt/U6N	1.73	24.34
Pt@U6N	1.81	87.24
PCs@U6N	1.20	151.48
Pt-U6N	1.38	8.81
PCs-U6N	0.63	16.17
CPU6N	0.48	6.66

Table S2. Summary of some MOF-based photocatalysts

Sample	Co-catalyst	Light source	Sacrificial reagent	Photosensitizer	H_2 evolution rate (μmol $g^{-1}h^{-1}$)	TON	Reference
PCs@U6N	Pt	Visible	TEOA	Er B	36830.0	598.67	This paper
Zr-MOF	Pt	Visible	TEOA	Er B	41396.4	161.7	1
Zr-MOF	Pt	Visible	Methanol	Er B	460	17.4	2
Zr-MOF	Pt	Visible	TEOA	Rh B	116.1	2.3	3
Zr-MOF	Pt	Visible		$[Ir(ppy)_2(bpy)]Cl$		90.9	4
Cr-MOF	Pt	Visible	TEOA	Rh B	580	7.5	5
Zr-MOF	Pt	Visible	Methanol	Arene dye	1528	400	6
Hf-MOF	Pd	Visible	TEOA	None	7550	482.5	7
Ti-MOF	Pt/Au	UV-Vis	TEOA	None	1743	69.38	8
In-MOF	Pt	UV-Vis	TEOA	None	341	4.5	9

The turnover number of per hour was calculated by the equation of TON = $n(H_2)/n(Pt)$ based on the content of Pt.

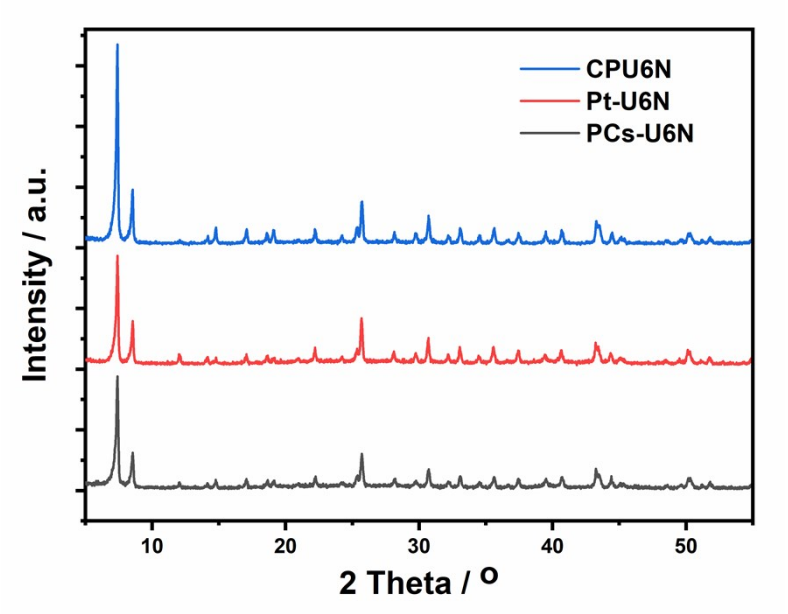

Figure S1. The PXRD patterns of PCs-U6N, Pt-U6N and CPU6N.

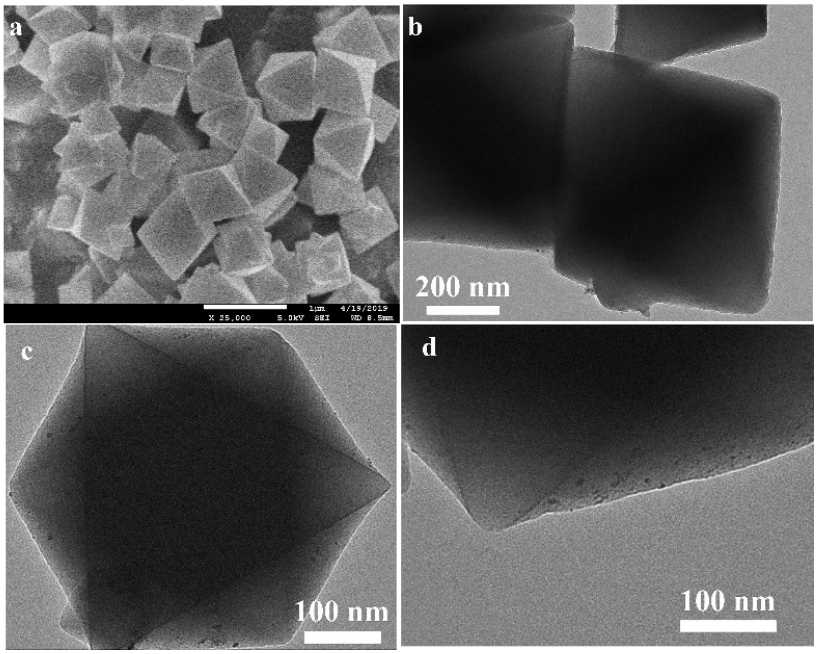

Figure S2. SEM image (a) and TEM images of PCs@U6N (b) and CPU6N (c and d).

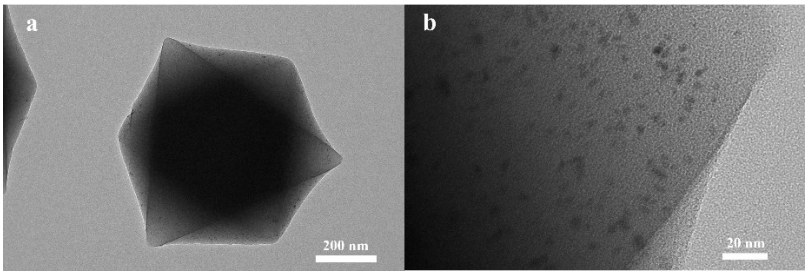

Figure S3. TEM images of PCs-U6N.

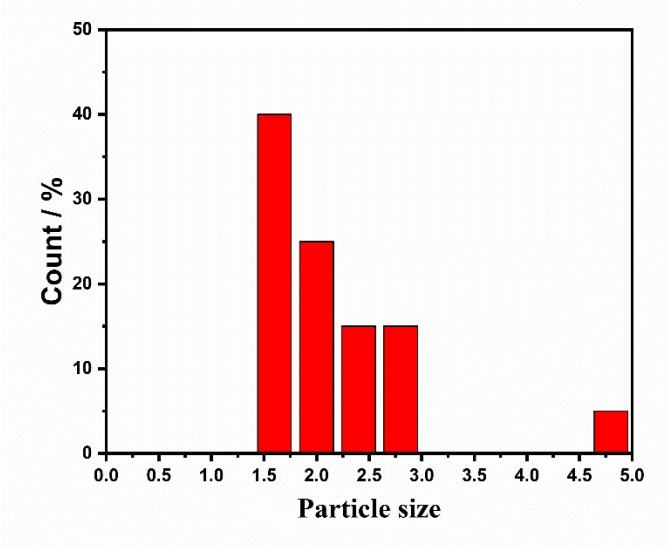

Figure S4. Pt nanoparticle size distribution in PCs-U6N.

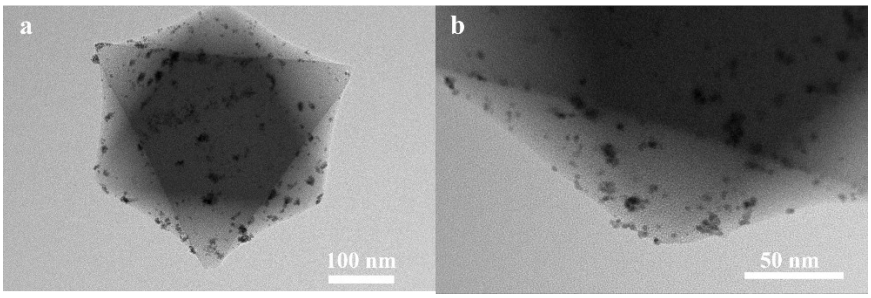

Figure S5. TEM images of Pt-U6N.

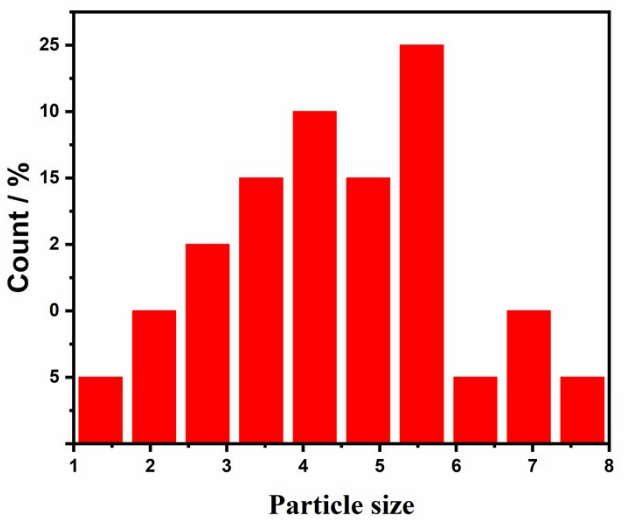

Figure S6. Pt nanoparticle size distribution in Pt-U6N.

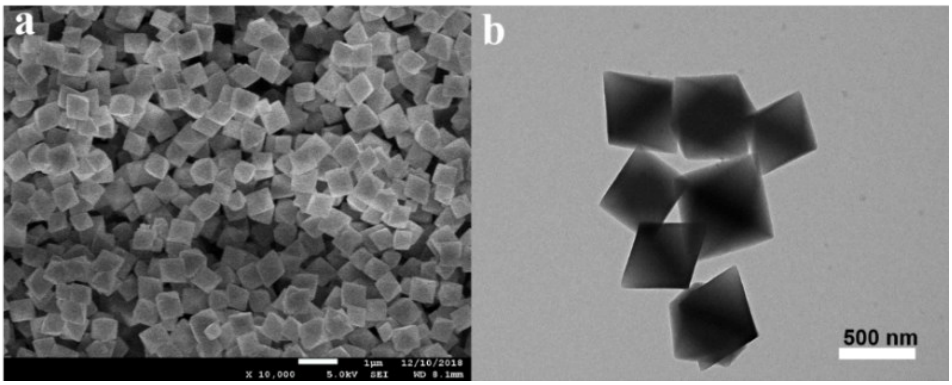

Figure S7. SEM image (a) and TEM image (b) of U6N.

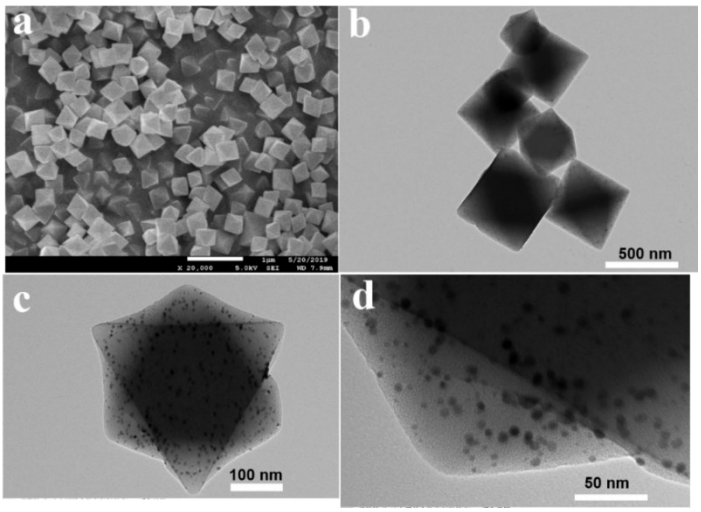

Figure S8. SEM image (a) and TEM images (b-d) of Pt@U6N.

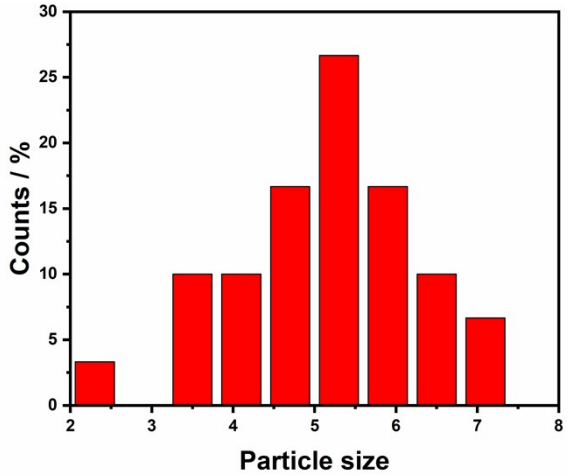

Figure S9. Pt nanoparticle size distribution in Pt@U6N.

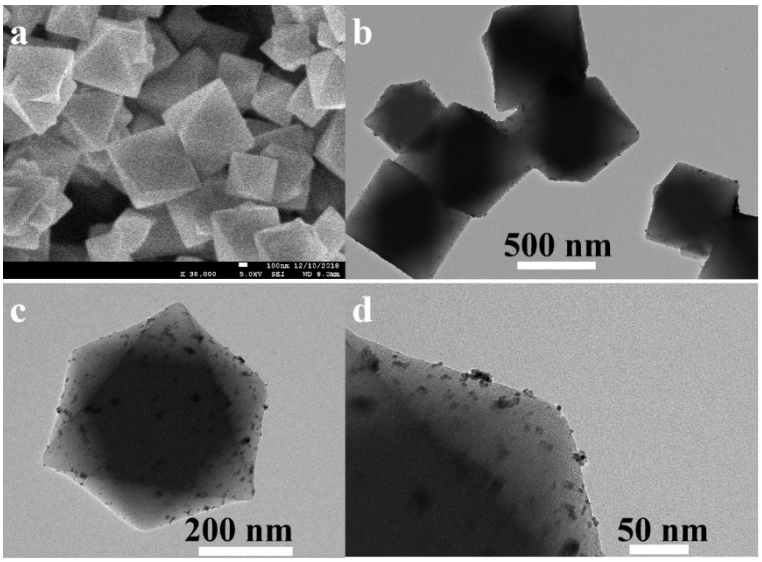

Figure S10. SEM image (a) and TEM images (b-d) of Pt/U6N.

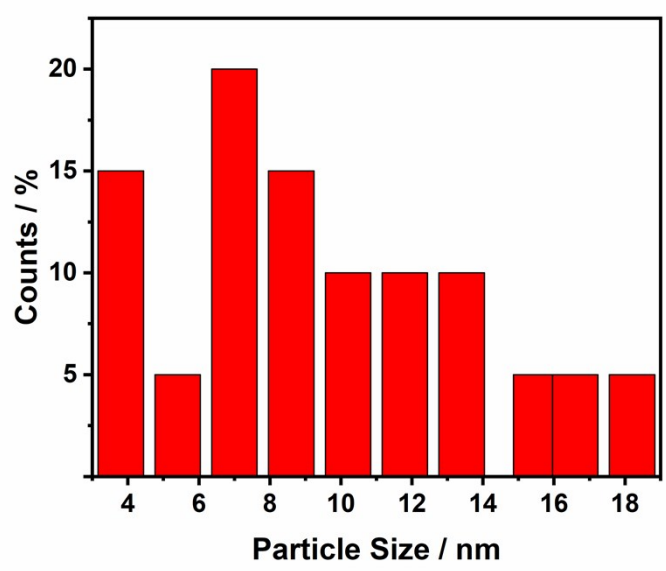

Figure S11. Pt nanoparticle size distribution in Pt/U6N.

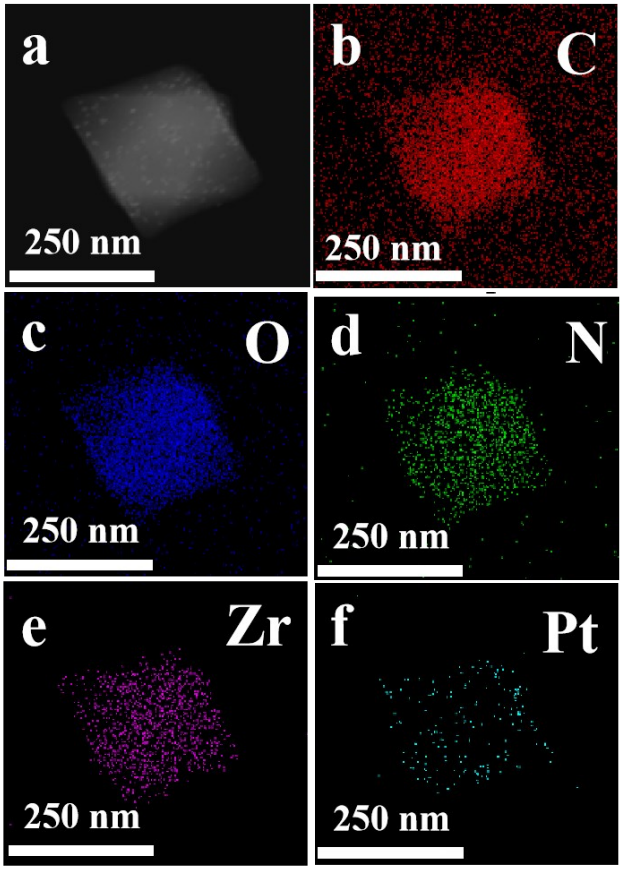

Figure S12. HAADF-STEM image (a) and element mapping images (b-f) of Pt@U6N.

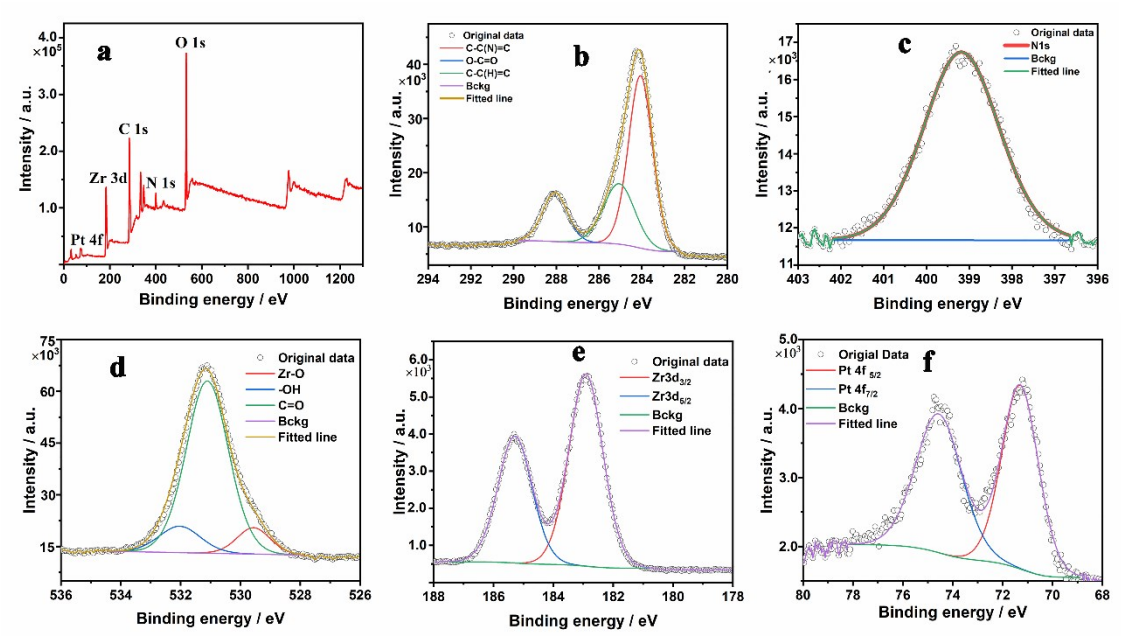

Figure S13. XPS survey spectrum (a) and high resolution XPS spectra of (b) C 1s, (c) N 1s, (d) O 1 s, (e) Zr 3d and (f) Pt 4f for Pt@U6N.

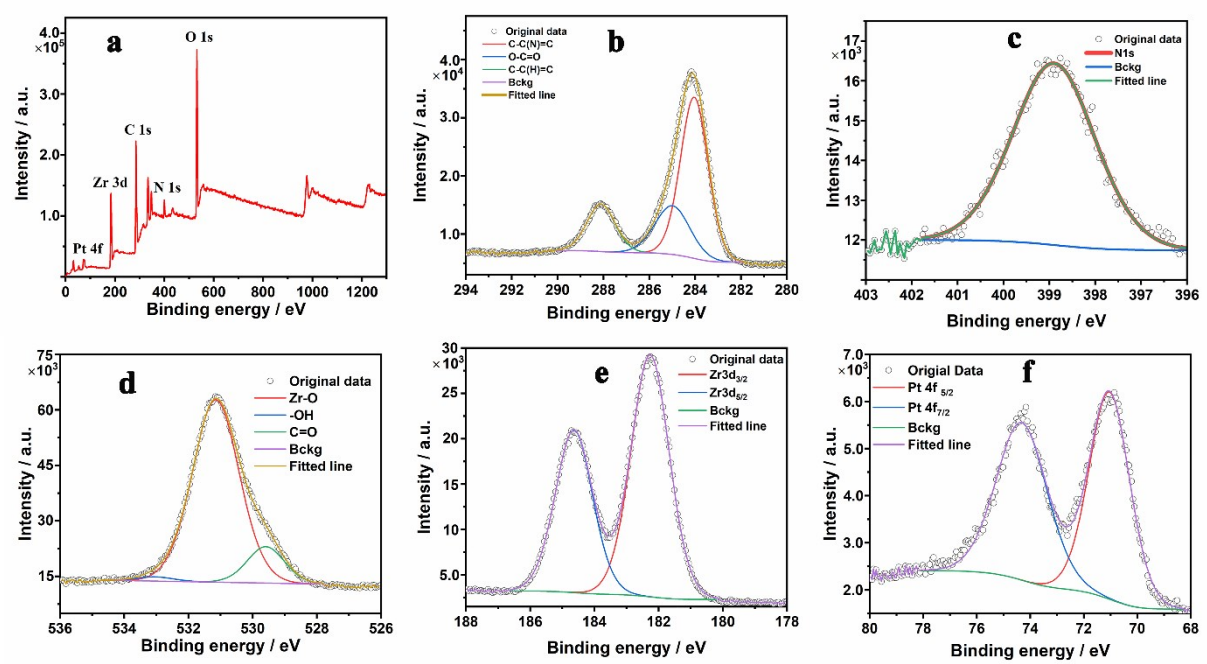

Figure S14. XPS survey spectrum (a) and high resolution XPS spectra of (b) C 1s, (c) N 1s, (d) O 1 s, (e) Zr 3d and (f) Pt 4f for Pt/U6N.

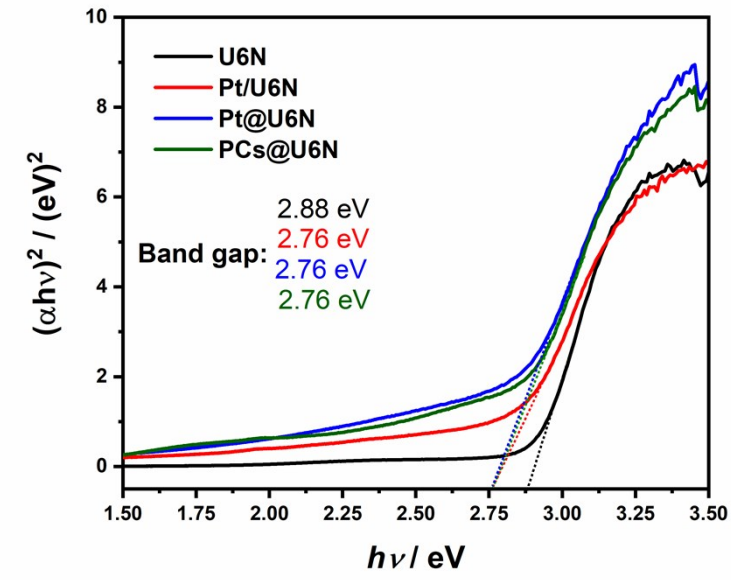

Figure S15. The band gap of U6N, Pt/U6N, Pt@U6N and PCs@U6N obtained through the Tauc plot method.

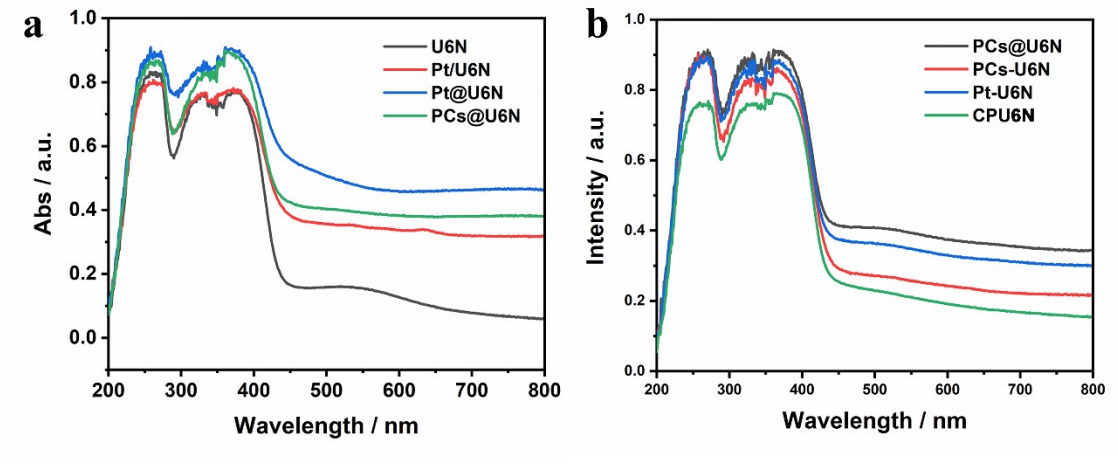

Figure S16. The repetitive UV-vis diffuse reflectance spectra of U6N, Pt/U6N, Pt@U6N and PCs@U6N after one month of the first test; the comparison of UV-vis diffuse reflectance spectra of PCs@U6N, PCs-U6N, Pt-U6N and CPU6N.

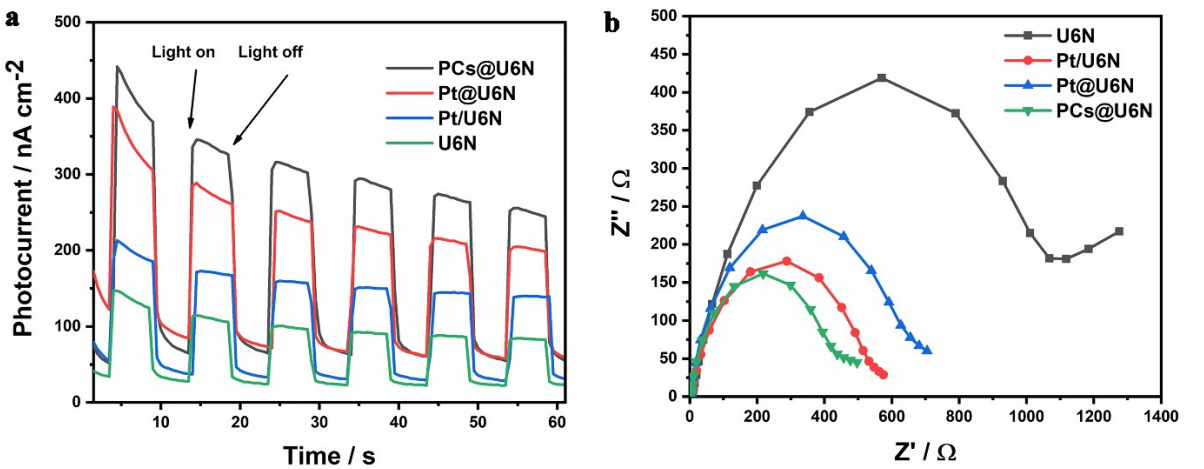

Figure S17. Photocurrent response and nyquist plots of electrochemical impedance spectroscopy (EIS) for PCs@U6N, Pt@U6N, Pt/U6N and U6N.

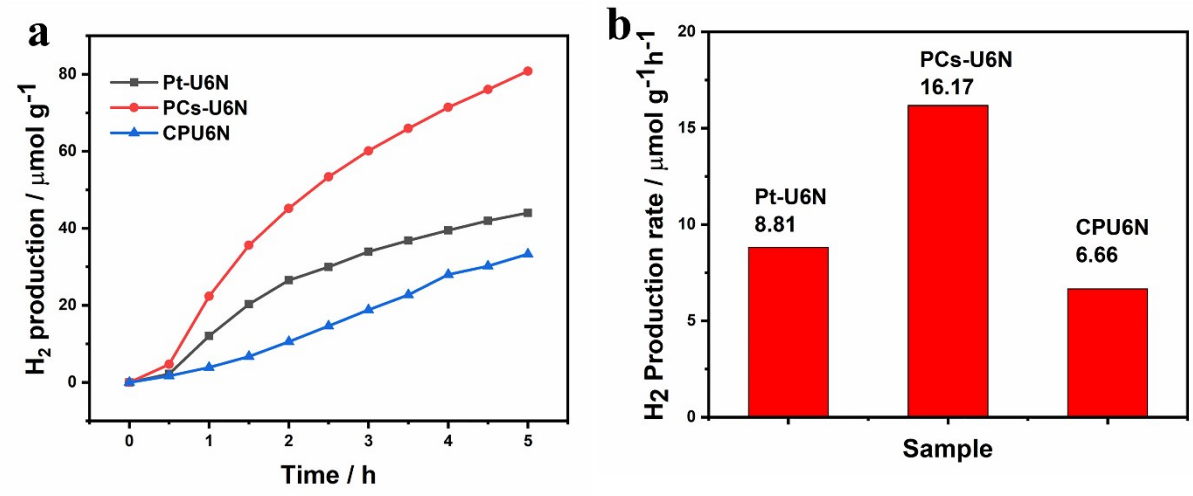

Figure S18. The photocatalytic hydrogen-production rates (a) of PCs-U6N, Pt-U6N and CPU6N; the performance comparison (b) of PCs-U6N, Pt-U6N and CPU6N.

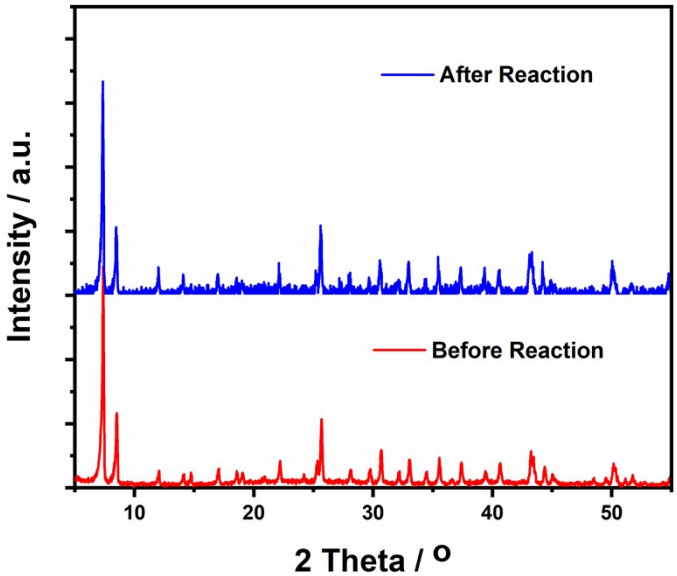

Figure 19. The PXRD patterns of PCs@U6N before and after HER reaction without Er B.

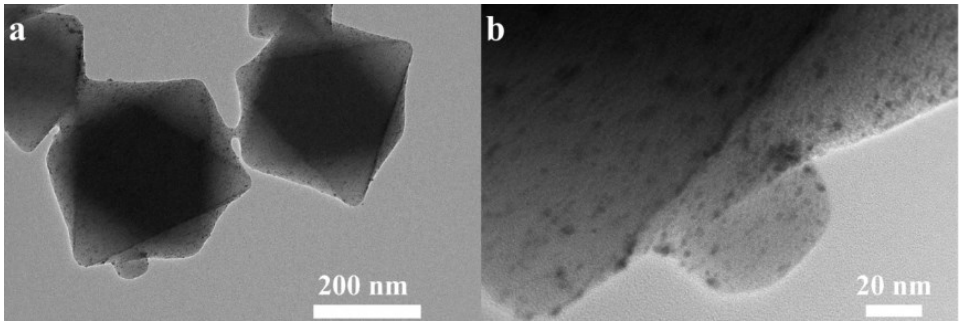

Figure 20. (a) The TEM image (a) and HRTEM image (b) of PCs@U6N after HER reaction without photosensitizer.

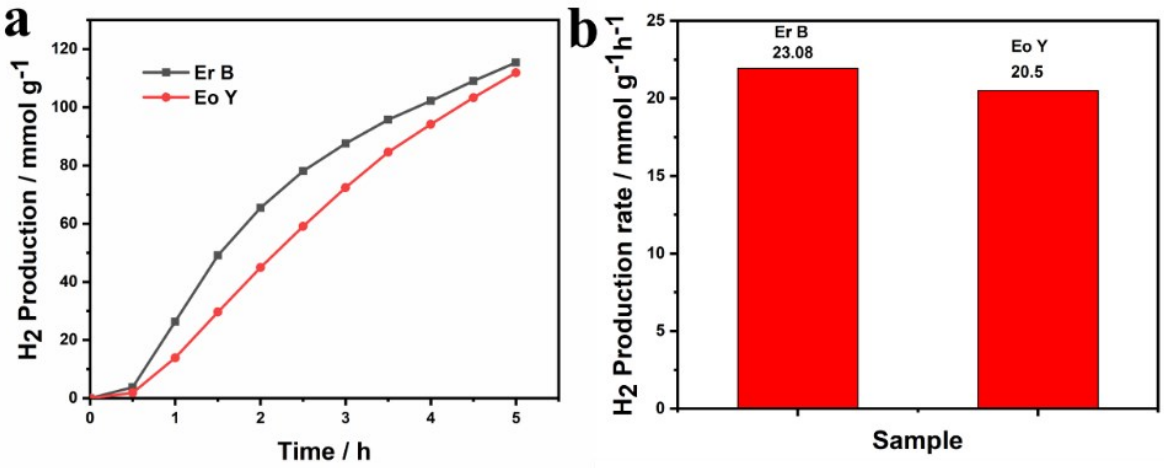

Figure S21. The photocatalytic hydrogen-production rates (a) of PCs@U6N with different molecular photosensitizer and performance comparison (b).

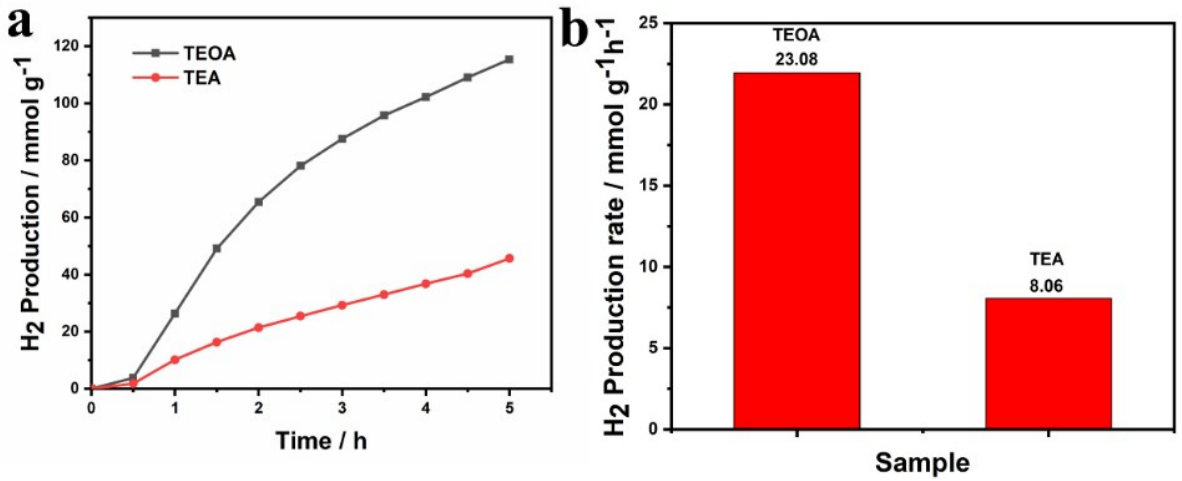

Figure S22. The photocatalytic hydrogen-production rates (a) of PCs@U6N with different sacrificial agent and (b) performance comparison.

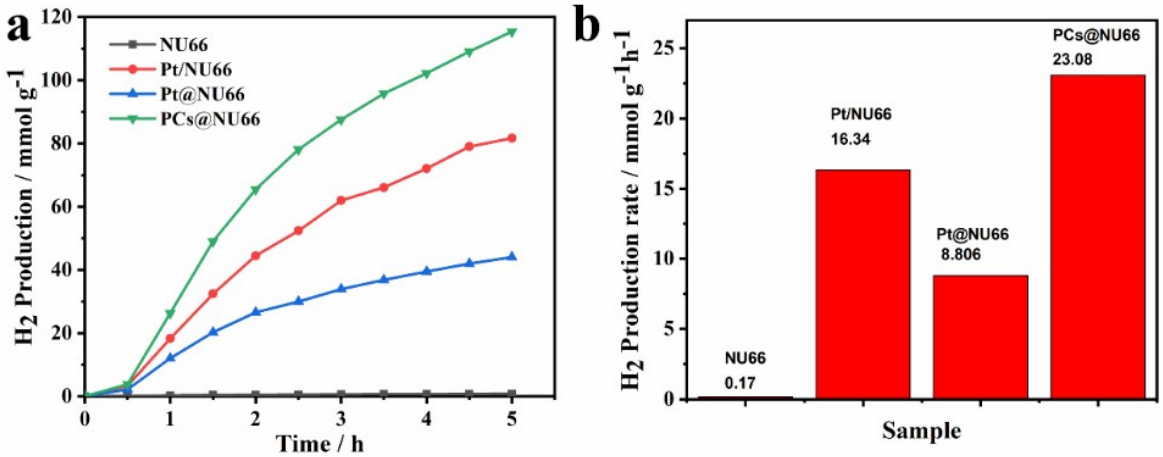

Figure S23. The photocatalytic hydrogen-production rates of PCs@U6N, Pt@U6N, Pt/U6N and U6N (a) and performance comparison (b) with a mass ratio (5:1) of catalyst to photosensitizer under visible light.

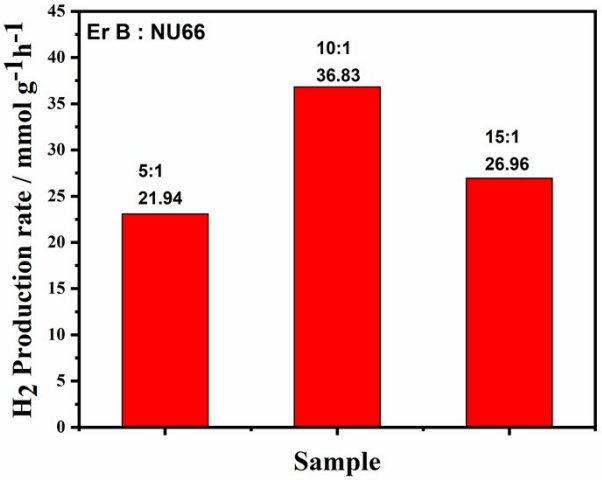

Figure S24. The photocatalytic hydrogen-production performance comparison of PCs@U6N with various amounts of Er B.

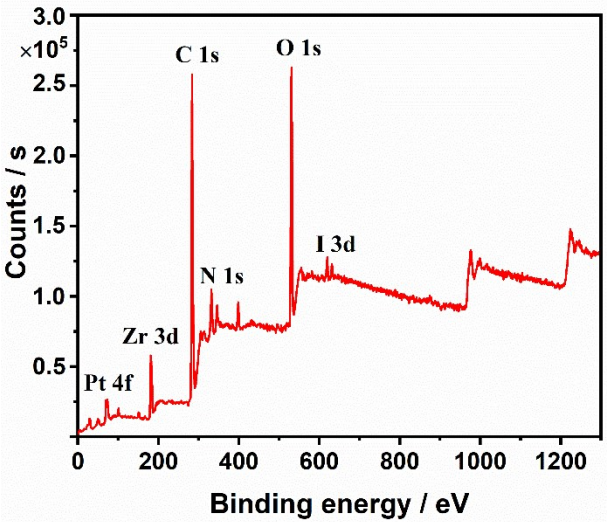

Figure S25. XPS spectrum of PCs@U6N after recycle used with photosensitizer.

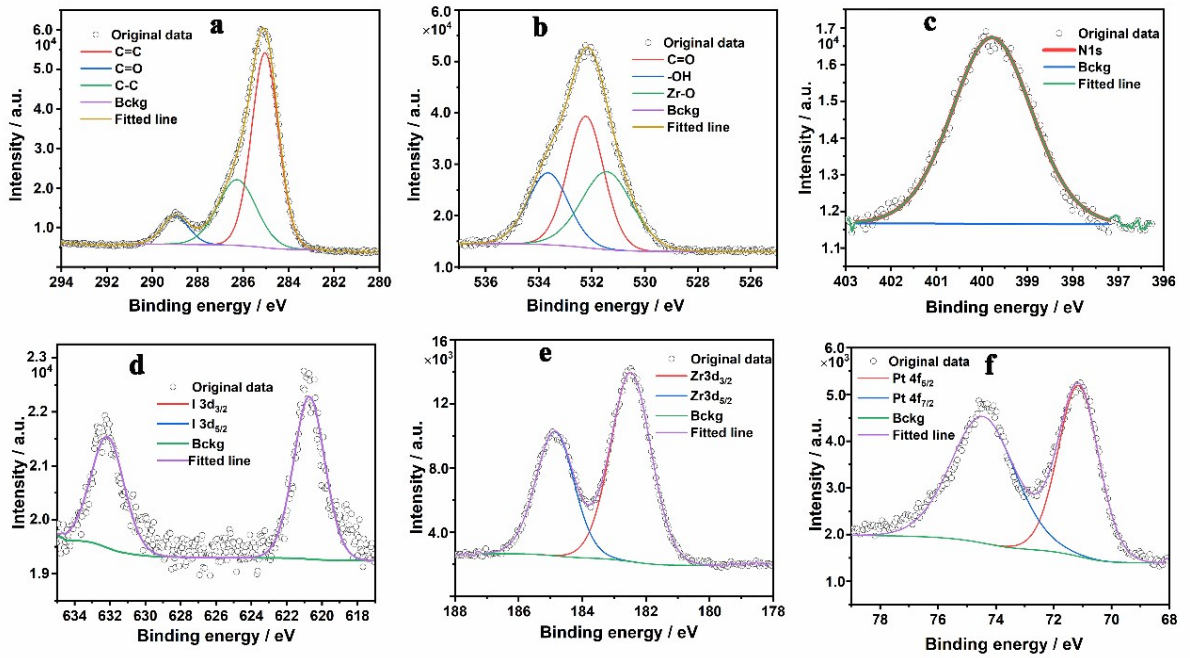

Figure S26. High-resolution C 1s (a), O 1s (b), N 1s (c), I 3d (d), Zr 3d (e) and Pt 4f (f) XPS spectrum of PCs@U6N after recycle used with molecular photosensitizer Er B.

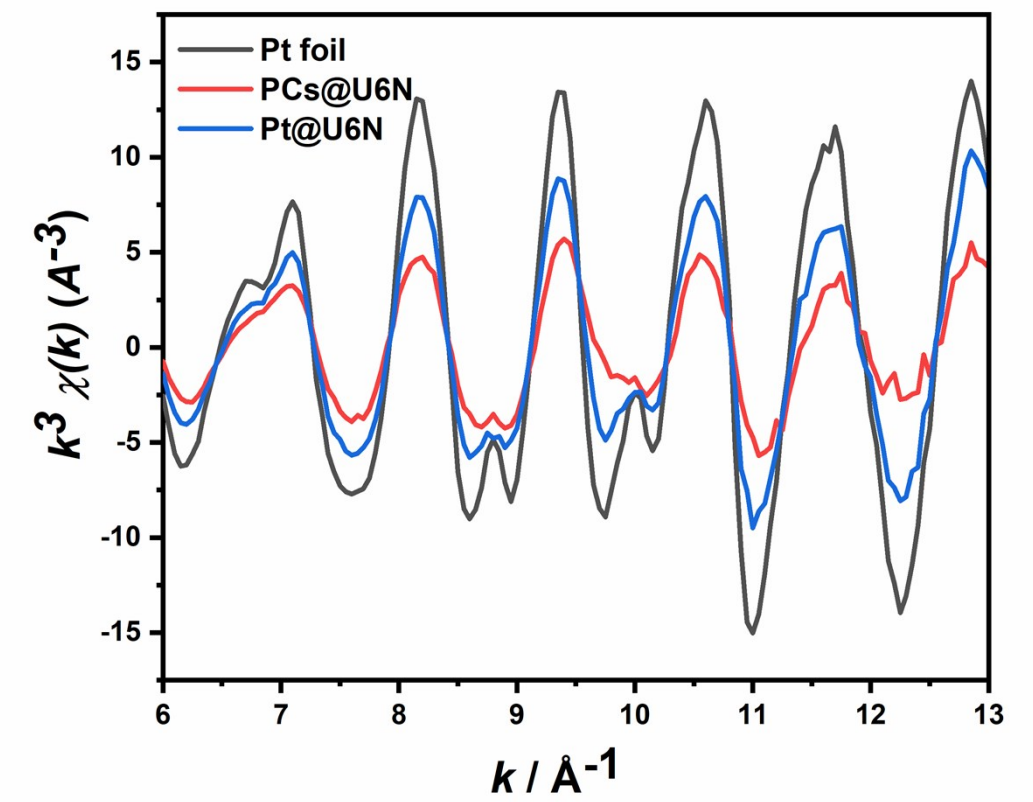

Figure S27. The Pt L_3-edge EXAFS of Pt foil, Pt@U6N and PCs@U6N in k spaces.

References

1 Y. Wang, Y. Yu, R. Li, H. Liu, W. Zhang, L. Ling, W. Duan, B. Liu, *J. Mater. Chem. A.* 2017, **5**, 20136.

2 Y.-P. Yuan, L.-S. Yin, S.-W. Cao, G.-S. Xu, C.-H. Li, C. Xue, *Appl. Catal. B* 2015, **572**, 168.

3 J. He, J.-Q. Wang; Y.-J. Chen, J.-P. Zhang D.-L. Duan, Y. Wang, Z. Yan, *Chem. Commun.* 2014, **50**, 7063.

4 C. Wang, K. E. deKrafft, W. Lin, *J. Am. Chem. Soc.* 2012, **134**, 7211.

5 M. Wen, K. Mori, T. Kamegawa, H. Yamashita, *Chem. Commun.* 2014, **50**, 11645.

6 Y.-F. Chen, L.-L. Tan, J.-M. Liu, S. Qin, Z.-Q. Xie, J.-F. Huang, Y.-W. Xu, L.-M. Xiao, C.-Y. Su, *Appl. Catal. B* 2017, **206**, 426.

7 S. Li, H.-M. Mei, S.-L. Yao, Z.-Y. Chen, Y.-L. Lu, L. Zhang, C.-Y. Su, *Chem. Sci.* 2019, **10**, 10577.

8 J. D. Xiao, L. Han, J. Luo, S. H. Yu, H. L. Jiang, *Angew. Chem. Int. Ed.* 2018, **57**, 1103.

9 F. Leng, H. Liu, M. Ding, Q.-P. Lin, H.-L. Jiang, *ACS Catal.* 2018, **8**, 4583-4590.